Korean J. Chem. Eng., **26**(6), 1556-1562 (2009)
DOI: 10.1007/s11814-009-0270-z

Characteristics and photocatalytic degradation of methyl orange on Ti-RH-MCM-41 and TiO_2/RH-MCM-41

Surachai Artkla*, Kitirote Wantala, Bang-orn Srinameb**, Nurak Grisdanurak**,***, Wantana Klysubun****, and Jatuporn Wittayakun*,***,†**

*Material Chemistry Research Unit, School of Chemistry, Institute of Science, Suranaree University of Technology, Nakhon Ratchasima, Thailand
**Department of Chemical Engineering, Thammasat University, Pathumthani, Thailand
***National Center of Excellence for Environmental and Hazardous Waste Management, Thammasat University, Pathumthani, Thailand
****Synchrotron Light Research Institute (Public Organization), Nakhon Ratchasima, Thailand
(*Received 19 February 2009 • accepted 29 April 2009*)

Abstract−Our purpose was to synthesize, characterize and test photodegradation of methyl orange on two catalysts containing 10 wt% titanium supported on mesoporous MCM-41 synthesized with rice husk silica. The first catalyst was Ti-RH-MCM-41 prepared by adding tetrabutyl orthotitanate (TBOT) in a synthetic gel of RH-MCM-41, and the second catalyst was TiO_2/RH-MCM-41 prepared by grafting TBOT on the preformed RH-MCM-41. The mesoporous structures were observed on both catalysts and they had surface area of 1,073 and 1,006 m^2/g. The Ti in Ti-RH-MCM-41 was in the form of Ti(IV) with tetrahedral geometry residing in the mesoporous structure. This form was less active for photodegradation of methyl orange than the other one. The Ti in TiO_2/RH-MCM-41 was anatase titania with octahedral geometry located outside the mesoporous framework. This form was more an active phase for the photodegradation and the reaction parameters on this catalyst were further investigated. The optimum catalyst weight to methyl orange volume ratio was 5 g/L and the optimum initial concentration of the dye was 2.0 ppm. The degradation rate obeyed pseudo-first order and the adsorption of methyl orange on TiO_2/RH-MCM-41 obeyed Langmuir isotherm.

Key words: Photocatalysis, RH-MCM-41, TiO_2, Methyl Orange, Photodegradation

INTRODUCTION

Dye stuff is routinely applied in various products and it can be hazardous to human health and environment because about 15% of the dye is lost during the production and application processes [1]. The release of dye effluent causes water contamination, which leads to pollution or dangerous by-products [2]. One process that can effectively remove hazardous dyestuffs is advanced oxidation processes (AOPs), which can generate active species including $^{\bullet}OH$, $^{\bullet-}O_2$ and $^{\bullet}O_2H$ to oxidize organic compound under UV light [3,4]. Titania or TiO_2 is a useful photocatalyst for AOPs because it is stable, active and inexpensive. Absorption of UV-vis energy on TiO_2 can excite electrons to conduction band (e^-_{CB}) and resulting positive holes in valence band (h^+_{VB}). The e^-_{CB} reduces O_2 or electron acceptor and h^+_{VB} oxidizes titanol groups (Ti-OH) or donator to generate hydroxyl radical ($^{\bullet}OH$). Finally, the $^{\bullet}OH$ can oxidize total organic compounds (TOC) to from TOC in oxidized species, H_2O and CO_2 [4].

Studies on photodegradation of azo dye on bare TiO_2 containing various functionalities in aqueous solution under UV irradiation have been reported [4]. The intermediates including oxygenates and acid compounds were monitored and they could be consecutively mineralized to downstream products. Nam and Han prepared nano-sized TiO_2 photocatalysts by solvothermal and hydrothermal methods and found that anatase was an active phase for photooxidation of methyl orange [5,6].

Problems that can decrease the photoactivity of TiO_2 are electron-hole recombination and particle aggregation, which can be overcome by dispersing TiO_2 on materials with high surface area. Bhattacharyya et al. [7] studied photodegradation of acid orange II on bare and supported TiO_2 on MCM-41, montmorillonite and zeolite beta under UV light. The catalysts were prepared by a sol-gel method or impregnation on various supports with the loading of 10-80 wt% of TiO_2. The photocatalytic efficiencies on supported catalysts were greater than that on bare TiO_2. Li et al. [8] used similar catalysts to study the pH dependence and found that the maximum photodegradation rate was achieved at the pH range of 4-5 for supported catalysts and was 2.5 times higher than the rate on unsupported TiO_2 (Degussa p25). The supported TiO_2 gave a higher degradation rate and needed a shorter reaction time because the active sites were increased by the dispersion. The improvement was reasoned to be by a better adsorption of acid II molecule on supported mesoporous MCM-41 that possesses a high surface area and narrow pore size distribution, providing accessibility for bulky molecules. Hydroxyl radicals on MCM-41 were believed to protect electron-hole recombination by trapping the generated holes that could react with the $^{\bullet}OH$ on catalyst surface [9]. In addition, it was reported that the addition of H_2O_2 with concentration of 0.01 M improved the photodegradation rate because it prevented electron-hole recombination by reacting with electron to produce hydroxyl radicals [8].

Previously, we reported the utilization of rice husk silica (RHS) in the syntheses of porous materials including MCM-41, zeolite X, Y

†To whom correspondence should be addressed.
E-mail: jatuporn@sut.ac.th

and Beta [10-13]. This work expanded the use of MCM-41 synthesized from RHS for photocatalytic application by adding titanium. The catalysts were prepared by two different methods. The first, noted as Ti-RH-MCM-41, was prepared by adding tetrabutyl orthotitanate (TBOT) in a synthetic gel of RH-MCM-41 to get Ti into the structural framework. The second catalyst, TiO_2/RH-MCM-41, was prepared by grafting TBOT on preformed RH-MCM-41 which contained Ti in extraframework. The physicochemical characteristics and performances on photodegradation of methyl orange of both catalysts were compared. Thus, in this study we aimed to compare the catalytic performance of TiO_2/RH-MCM-41 and Ti-RH-MCM-41 in the presence of 0.01 M H_2O_2 as electron acceptor. The reaction parameters were also studied.

EXPERIMENTAL

1. Chemicals and Materials

Chemical for silica extraction from rice husk was hydrochloric acid (37% HCl, Carlo Erba). Chemicals for the syntheses of RH-MCM-41 and Ti-RH-MCM-41 were tetrabutylorthotitanate (TBOT, 99% $C_{16}H_{36}O_4Ti$, Acros), cetyltrimethylammonium bromide or CTAB (96% $C_{19}H_{42}NBr$, Fluka), rice husk silica (SiO_2 with 98% purity [10, 12], sodium hydroxide (97% NaOH, Carlo Erba) and sulfuric acid (96% H_2SO_4, Carlo Erba). Chemicals for the preparation of TiO_2/RH-MCM-41 and photocatalytic degradation were RH-MCM-41, TBOT, nitric acid (65% HNO_3, Carlo Erba), NaOH and methyl orange (Riedel-de Haen).

2. Preparation of RHS

Rice husk was obtained from local rice milling and silica preparation was via acid-leaching method similar to our previous works [11,12]. The rice husk was thoroughly washed with water, dried at 100 °C overnight, refluxed with 3 M HCl for 6 h, filtered and washed several times with water until the filtrate was neutral and dried at 60 °C overnight. The obtained black solid product was pyrolyzed in a muffle furnace at 550 °C for 6 h to remove the organic contents to produce RHS.

3. Synthesis of RH-MCM-41

RH-MCM-41 synthesis was modified from a procedure described in the literature [10,14] by using RHS and hydrothermal method with a gel molar ratio of $1.0SiO_2$: 0.25CTABr: $180H_2O$. First, CTAB (1.45 g) was dissolved in deionized water (30.00 mL), stirred for 4 h to obtain a clear solution, denoted as solution A. Solution B was simultaneously prepared by dissolving rice husk silica (1.00 g) and NaOH (2.00 g) deionized water (15 mL) with a constant stirring for 4 h to obtain a clear solution. Then solution A was poured into a 100-mL teflon container and solution B was gradually added dropwise within 20 min. The mixture pH was adjusted to 11.5 by slowly dropping 5 N H_2SO_4 until small agglomerated particles started to form. The gel mixture was then transferred into a teflon-lined autoclave and crystallized at 100 °C for 72 h. The product mixture was filtered, dried at 100 °C, ground and calcined at 540 °C to remove the template. The products denoted as RH-MCM-41 were characterized by X-ray diffraction (XRD) and nitrogen adsorption-desorption analysis.

4. Synthesis of Ti-RH-MCM-41

The Ti-RH-MCM-41 with 10 wt% of titania was synthesized from CTAB, TBOT and RHS dissolved in 3.33 M NaOH solution with a gel molar ratio of $1.0SiO_2$: 0.05TBOT : 3.0NaOH : 0.25CTAB : $180H_2O$ [10,14]. The pH was adjusted to 11.5 and the mixture was crystallized at 100 °C for 72 h in a teflon-lined autoclave. Then the as-prepared Ti-RH-MCM-41 was filtered, dried by deionized water several times, aged overnight and calcined at 540 °C for 6 h. The obtained white powder of Ti-RH-MCM-41 was characterized by XRD, nitrogen adsorption-desorption analysis and X-ray absorption spectroscopy (XAS).

5. Preparation of TiO_2/RH-MCM-41

The preparation of TiO_2 sol was by an acid catalyzed sol-gel formation method modified from the literature [7]. First, an appropriate amount of TBOT to produce 10 wt% titania was added gradually to an aqueous solution of 1 M HNO_3 acid (40 mL) under continuous stirring for 1.5-2 h to produce a transparent sol. Subsequently, the mixture was diluted with deionized water and the pH was adjusted to 3 with 1 M NaOH to give a turbid colloid. The required amount of RH-MCM-41 to produce 10%TiO_2/RH-MCM-41 was added to the turbid colloid suspension. The resulting mixed suspension was agitated by a magnetic stirrer for another 2 h at room temperature, separated by centrifugations and washed several times with deionized water until the pH of the filtrate was about 6. The resulting TiO_2/RH-MCM-41 was dried overnight in an oven and calcined in furnace at 300 °C for 1 h.

6. Catalysts Characterization

The crystalline phase of RH-MCM-41, TiO_2/RH-MCM-41 and Ti-RH-MCM-41 were analyzed by using powder XRD (Bruker axs D5005 diffractometer) with Cu K_α radiation.

X-ray absorption spectra of Ti-RH-MCM-41 and references compounds were measured in the energy region of the titanium K-edge (4,966 eV) in transmission mode at the beamline BL-8 of Synchrotron Light Research Institute (Public Organization). The X-rays were emitted from an electron storage ring operating at 1.2 GeV and diffracted with a Si(111) two-crystal monochromator. X-ray absorption near edge structure (XANES) spectra were normalized with the Athena program, the edge shifts were corrected to standard reference compounds to determine characteristics of the sample.

Nitrogen adsorption-desorption isotherms were measured at liquid nitrogen temperature from a relative pressure of 0.01 to 0.99 on a Micromeritics ASAP 2010. Before the measurement, each sample was degassed at 250 °C for 3 h. The surface areas were obtained from the adsorption data in the relative pressure range of 0.02-0.2 by BET method. The pore size and pore volumes were calculated from the desorption branches of the isotherm by BJH method.

7. Catalytic Testing for Photocatalytic Degradation of Methyl Orange

The tests were conducted in a photochemical reactor at room temperature. First the performances of Ti-RH-MCM-41 and TiO_2/RH-MCM-41 were compared with a ratio between the catalyst weight and methyl orange volume of 2.5 g/L and initial methyl orange concentration of 2 ppm. A solution of H_2O_2 (30% w/v) was added to the mixture to produce 0.01 M H_2O_2 in the solution and stirred in a dark chamber for 30 min prior to illumination with a UV lamp (10 W). To investigate the changes of reaction, samplings were done at 0, 5, 10, 15, 20 and 30 min. The decrease of methyl orange concentration in the solution was determined by a UV-VIS (Shimadzu, UV 1201) spectrometer. The catalyst with a better performance was

tested for the effect of catalyst weight to methyl orange solution including 1.0, 2.5, 5.0 and 7.5 g/L when the concentration of methyl orange was fixed at 2.0 ppm in all mixtures. The catalyst with optimum ratio was tested further with various methyl orange concentrations, including 2.0, 4.0, 6.0 and 8.0 ppm.

8. Adsorption of Methyl Orange on TiO_2/RH-MCM-41

To study the adsorption of methyl orange on TiO_2/RH-MCM-41, various methyl orange concentrations, 2.0, 4.0, 6.0 and 8.0 ppm, were prepared and mixed with TiO_2/RH-MCM-41 in an erlenmeyer flask to give catalyst weight to methyl orange volume ratio of 5.0 g/L. The mixture was stirred vigorously in the dark for 30 min to establish equilibrium adsorption. Then, the liquid product was sampled to analyze by the UV-Vis spectrometer. The decreases of methyl orange concentrations were plotted versus absorbance to reveal adsorption isotherm of methyl orange on the solid catalyst.

RESULTS AND DISCUSSION

1. Catalyst Characterization

The purity of rice husk silica (RH-SiO_2) analyzed by X-ray fluorescence was 98% with traces of alumina, potassium oxide and calcium oxide [11,12].

XRD patterns of TiO_2/RH-MCM-41 and Ti-RH-MCM-41 are shown in Fig. 1(a). Although they were prepared differently, they gave similar XRD patterns with four characteristic peaks of (100), (110), (200) and (211) planes that confirmed an ordered structure as in the parent MCM-41 [15]. Thus, incorporating Ti into the structure of RH-MCM-41 by adding TBOT into the synthetic gel and grafting TBOT on the preformed RH-MCM-41 did not cause much change in the MCM-41 structure.

In the calcined Ti-RH-MCM-41, characteristic peaks of either rutile or anatase phase of TiO_2 were not observed by XRD. The nature of Ti in this sample was investigated further by XANES. In contrast, anatase phase was observed in the XRD spectrum of TiO_2/RH-MCM-41 at 2θ of 25.3 degree (Fig. 1(b)).

Normalized Ti K-edge XANES spectrum of Ti-RH-MCM-41 along with TiO_2 anatase and Ti foil references are shown in Fig. 2. The pre-edge, small peak(s) before the sharp rise in the spectrum is a result of the excitation of the core electron of Ti to empty bound states and depends on atomic geometry [16]. Titanium foil showed only one strong pre-edge peak at 4,967.9 eV, which is a characteristic of tetrahedral symmetry. The spectrum of anatase standard showed three low intensity pre-edge peaks at 4,968.1, 4,964.6 and 4,970.4 eV, which are the characteristic of octahedrally coordinated titanium atoms [17]. The spectrum of Ti-RH-MCM-41 sample exhibited a single pre-edge peak at 4,977.8 eV, which is a characteristic of the framework tetrahedrally coordinated titanium (IV) [18]. The peak shifted from the Ti foil because of the charge difference. The XANES results confirmed that Ti in Ti-RH-MCM-41 was not in anatase form.

The nitrogen adsorption-desorption isotherms of RH-MCM-41, Ti-RH-MCM-41 and TiO_2/RH-MCM-41 are compared in Fig. 3(a). They all gave type-IV isotherm with three well-defined stages similar to isotherms of RH-MCM-41 in the literature [10]. The adsorption in the first step from the beginning to a relative pressure around 0.2 concaved to the P/P_0 axis was attributed to monolayer adsorption

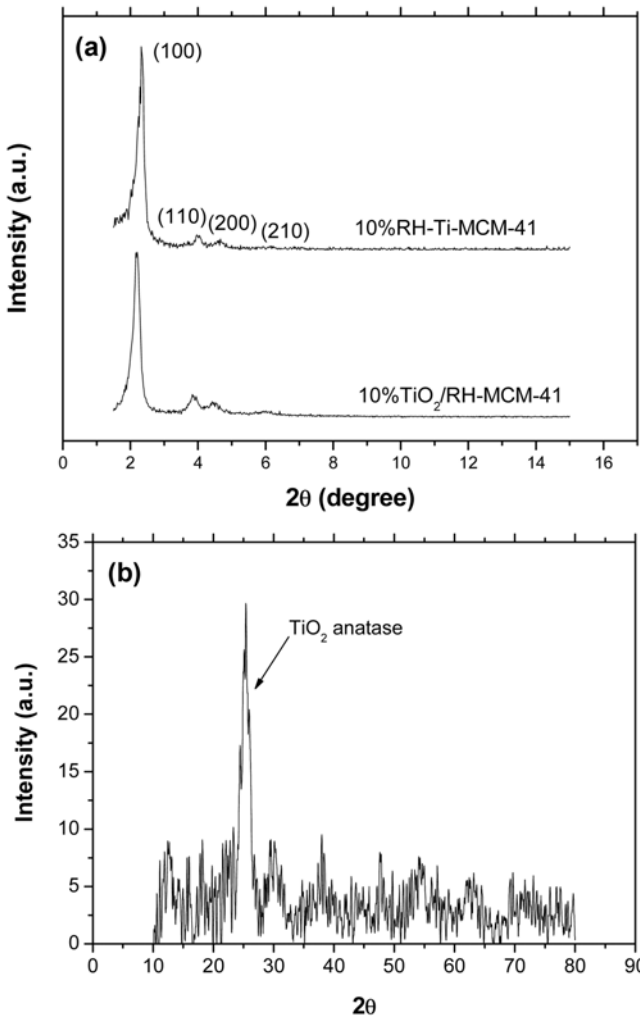

Fig. 1. (a) Low angle XRD patterns of Ti-RH-MCM-41 and TiO_2/RH-MCM-41 and (b) high angle XRD pattern of TiO_2/RH-MCM-41.

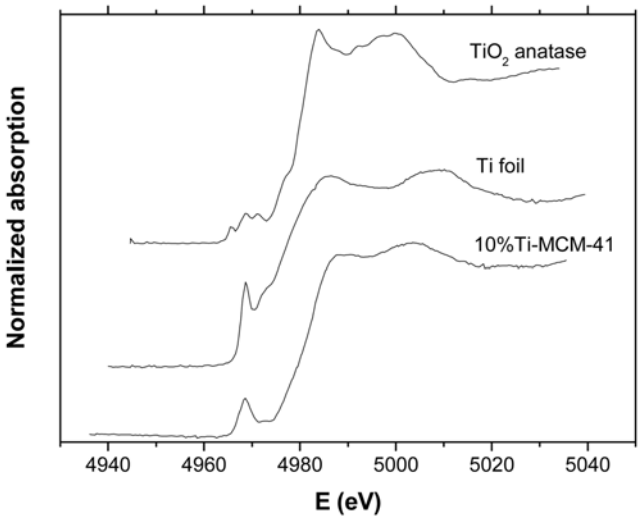

Fig. 2. Ti K-edge XANES spectra of Ti-RH-MCM-41, Ti foil and TiO_2 anatase references.

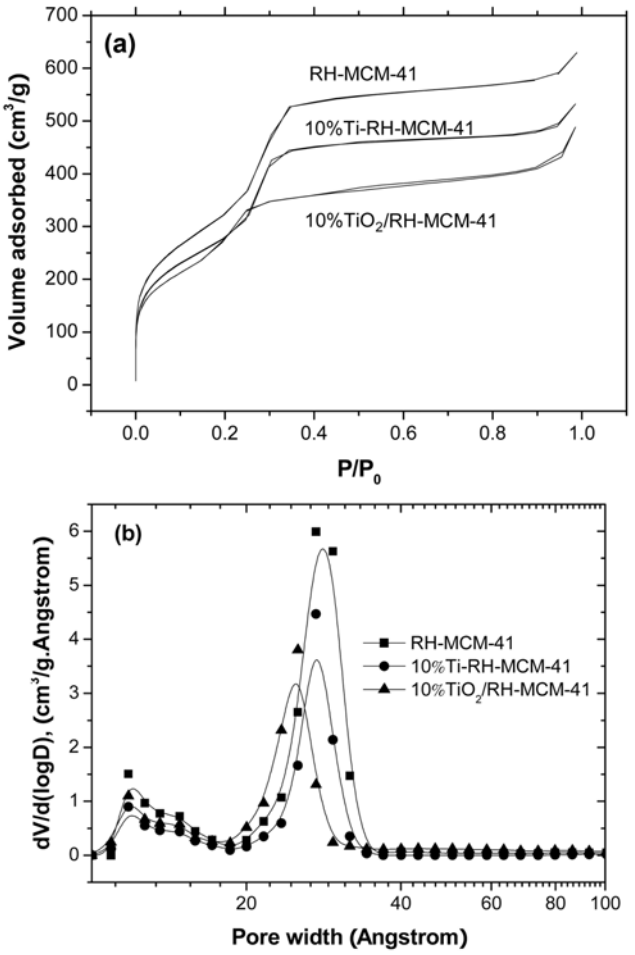

Fig. 3. (a) N_2 adsorption-desorption isotherm and (b) pore size distribution of RH-MCM-41 and Ti-RH-MCM-41.

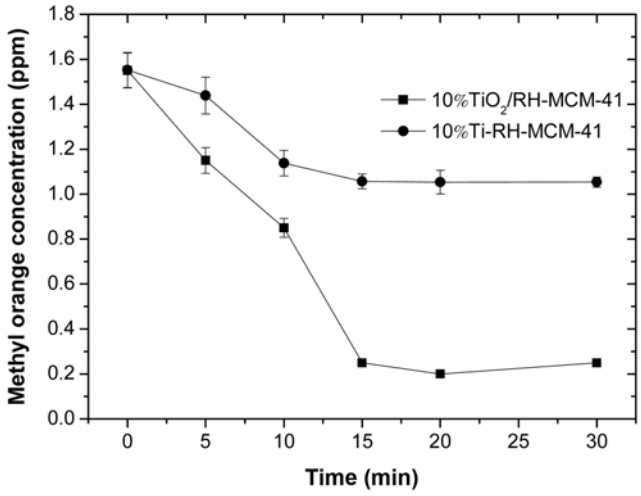

Fig. 4. Catalytic activity of Ti-RH-MCM-41 and Ti-MCM-41: [cat.] =2.5 g/L, C_0=2 ppm, pH=4.5, [H_2O_2]=0.01 M.

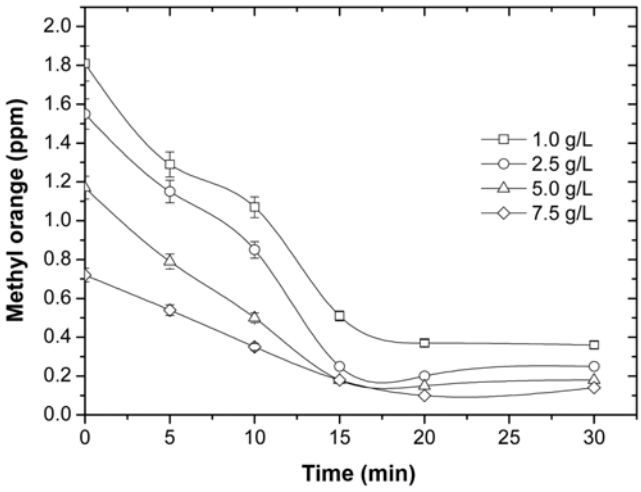

Fig. 5. Effect of catalyst concentration on photocatalytic degradation of methyl orange on TiO_2/RH-MCM-41: C_0=2 ppm, pH=4.5, [H_2O_2]=0.01 M.

on external surface. The lower adsorption volume on Ti-RH-MCM-41 and TiO_2/RH-MCM-41 indicated lower surface area. The specific surface area of RH-MCM-41, Ti-RH-MCM-41 and TiO_2/RH-MCM-41 was 1,231, 1,074 and 1,006 m^2/g, respectively. The adsorption at relative pressure of 0.2-0.4 was from adsorption in mesopores which were used to determine pore sizes.

The pore size distribution in RH-MCM-41, Ti-RH-MCM-41 and TiO_2/RH-MCM-41 is presented in Fig. 3(b), showing both micropores and mesopores. The plot showed the relationship between volume adsorbed and pore diameter (D) ratio in the pattern of differentiate operator (d). Large portions of mesopores were presented in all samples with diameter of 28.2, 27.4 and 24.9 Å in RH-MCM-41, Ti-RH-MCM-41 and TiO_2/RH-MCM-41, respectively.

2. Photodegradation of Methyl Orange

2-1. Catalytic Performance of Solid Catalysts

The decreases of methyl orange concentration from photocatalytic degradation on TiO_2/RH-MCM-41 and Ti-RH-MCM-41 are shown in Fig. 4. The photoactivity on TiO_2/RH-MCM-41 was better than that on Ti-RH-MCM-41 at every sampling time and the conversions after 20 min were 87.1% and 32.3% respectively. The higher activity was obtained because the form of TiO_2 in the TiO_2/RH-MCM-41 was anatase, which is a suitable form for photoreaction. The anatase phase could provide hydroxyl radicals for photooxidation of organic pollutants [9]. From this point forward, only TiO_2/RH-MCM-41 was studied to understand role of parameters and nature of the dye adsorption. The presence of TiO_2 was important as reported by Li et al. that less than 10% orange II was degraded in presence of only H_2O_2 and UV without TiO_2 [8].

2-2. Influence of Added Amount of Catalysts

Various weights of the TiO_2/RH-MCM-41 catalyst were added to a solution containing 2.0 ppm of methyl orange to produce concentrations of 1.0, 2.5, 5.0 and 7.5 g/L for the determination of the optimum catalyst concentration. The results are shown in Fig. 5. At the beginning, the initial concentrations were different because methyl orange adsorbed on the catalyst surface. The amount adsorbed increased with the catalyst concentration. The concentration of methyl orange in each test decreased linearly with time and became constant after 17 min. The degradation ratio increased with increasing of catalyst concentration along with reaction time until the concentration reached 5.0 g/L. With a further increase of cata-

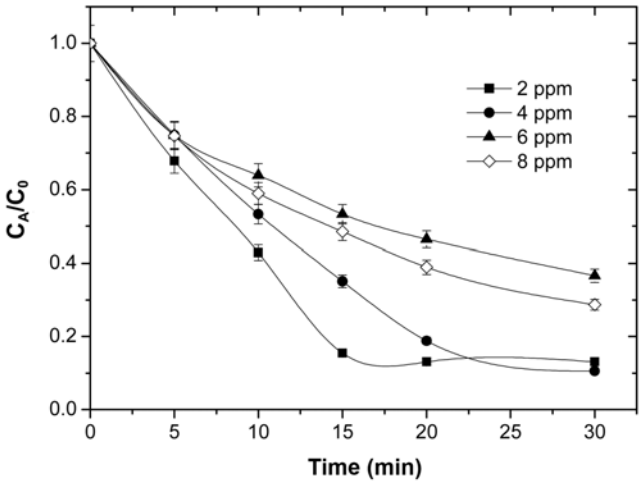

Fig. 6. Effect of methyl orange concentration to photocatalytic degradation on TiO_2/RH-MCM-41: [cat.]=5.0 g/L, pH=4.5, [H_2O_2]=0.01 M.

lyst concentration, degradation ratio was not significantly different because of the fact that larger suspension catalysts might block UV light and sequentially decreased hydroxyl radical, which were active species for photodegradation [4]. Moreover, the decrease in the percentage of degradation at higher catalyst loading might be caused by a deactivation of activated molecules by collision with ground state molecules [2]. Thus, the results suggested an optimal 5.0 g/L of TiO_2/RH-MCM-41 to achieve the most effective degradation of methyl orange. From this point forward, only the catalyst concentration of 5.0 g/L was used in the rest of the study.

2-3. Influence of Initial Concentration of Methyl Orange

The influence of the initial concentration of methyl orange on its photodegradation was studied by using the concentration of 2, 4, 6 and 8 ppm. The plot between C_A/C_0 (Where C_A and C_0 were the concentration of methyl orange at the sampling time and at the beginning, respectively) with time is shown in Fig. 6. The lower initial concentration gave higher degradation efficiency.

There are two possible reasons to explain the above result. First, a certain amount of TiO_2/RH-MCM-41 produces a certain amount of hydroxyl radical. When all H_2O_2 was consumed, the generation of hydroxyl radical was stopped and the active species to initiate reaction were no longer formed. Second, a higher concentration of methyl orange would adsorb and cover the catalyst surface and resulted in deactivation [1]. In the next experiment, only the initial concentration of 2 ppm was used to determine the reaction rate law because the equilibrium could be obtained in a short time.

2-4. Photodegradation Rate of Methyl Orange

The rate of reaction was assumed to be proportional to concentrations of the reactant. The plot between $-R_{CA}$ and C_A (Fig. 7(a)) demonstrated that the initial rate of reaction increased exponentially with the initial concentration of methyl orange. At the beginning, there were plenty of active species to propagate the reaction including hydroxyl radicals and adsorbed methyl orange. Thus, the degradation rate of methyl orange increased rapidly. After hydroxyl radicals were exhausted, there were only adsorbed methyl orange species on the catalyst; consequently, the degradation rate decreased.

In addition, the reaction rate constant was determined for the initial

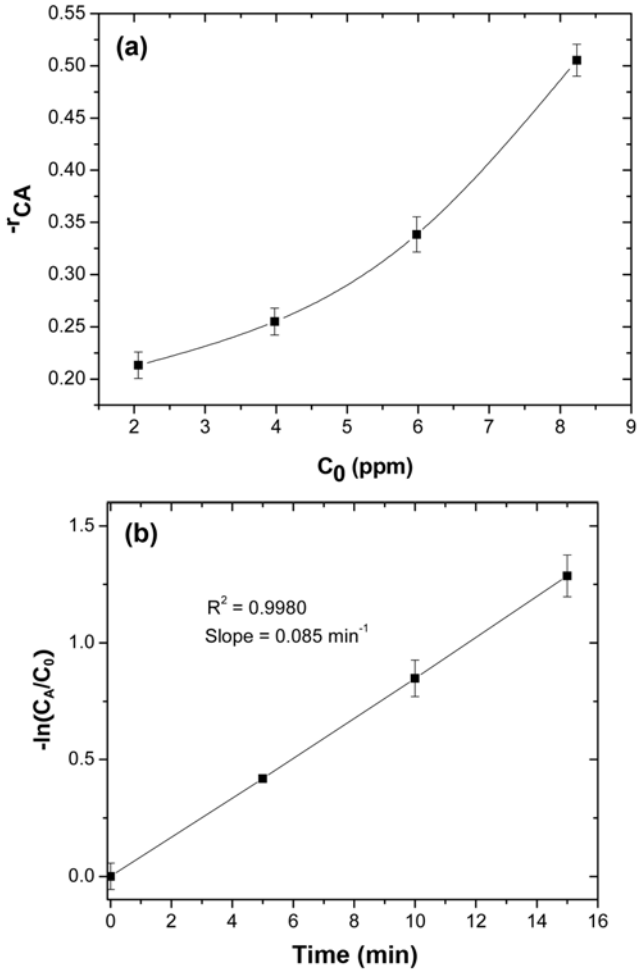

Fig. 7. (a) Dependence of initial degradation rate of methyl orange with initial concentration and (b) pseudo-first order plot of photocatalytic degradation of methyl orange with initial concentration of 2 ppm on TiO_2/RH-MCM-41.

concentration of 2 ppm from Eq. (1), which showed a relationship between $-\ln(C_A/C_0)$ and reaction time.

$$-\ln(C_A/C_0)=kt \quad (1)$$

$$t_{1/2}=\frac{0.693}{k} \quad (2)$$

From Fig. 7(b), the fit gave a straight line with R^2 of 0.9980. The slope of the linear relationship was reaction rate constant (k) which was 0.085 min^{-1}. This result indicated that the photocatalytic degradation methyl orange obeyed the pseudo-first order. The rate constant from initial concentration of 2 ppm was also calculated by half-life method as described in Eq. (2) using the data in Fig. 6. The obtained value was 0.082 min^{-1} and in good agreement with the first method.

2-5. Adsorption of Methyl Orange on TiO_2/RH-MCM-41

Adsorption of methyl orange on TiO_2/RH-MCM-41 was studied by stirring the mixture of methyl orange and catalyst in the dark and sampling clear solution after 0.5 h. The adsorption isotherms in this study were done by extrapolating with both Langmuir (Eq. (3)) and Freundlich isotherm (Eq. (4)). The obtained data were plotted corre-

sponding to both models and only the result with a linear fit was shown.

$$\frac{C_e}{q_e} = \frac{C_e}{q_{max}} + \frac{1}{K_{ad} \times q_{max}} \quad (3)$$

$$\log(q_e) = \log(K) + \frac{1}{n}\log(C_e) \quad (4)$$

Where:

C_e=equilibrium concentration of methyl orange in solution (mg/L)

q_e=amount of adsorbed methyl orange on catalyst at equilibrium concentration (mg/g)

q_{max}=maximum adsorption amount (mg/g)

K_{ad}=apparent adsorption equilibrium concentration $(mg/L)^{-1}$

K=adsorption capacity constant $(mg/L)^{-1}$

N=adsorption layer of methyl orange

In a simple adsorption explained by Langmuir isotherm, the chemical interaction between methyl orange and active sites on the catalyst surface produces monolayer adsorption. Each site is assumed to be independent from its neighboring sites. If the interaction is complicated with both physical and chemical interaction, multilayer adsorption is formed and the adsorption can be explained by Freundlich isotherm.

The plot between C_e/q_e and C_e, shown in Fig. 8 gave a straight line linear fit with R^2 of 0.9988, demonstrating that the adsorption amount of methyl orange increased with the initial concentration of methyl orange. The plot fit well with Langmuir isotherm, indicating that adsorption of methyl orange on TiO_2/RH-MCM-41 was monolayer. This agreed with previous adsorption study of methyl orange on bare TiO_2 which obeyed Langmuir isotherm [4]. There was no independent interaction with surrounding molecules. From Eq. (4), the maximum adsorption amount (q_{max}), calculated from the slope, was 0.18 mg/g. Furthermore, the adsorption constant (K_{ad}), calculated from q_{max} and Y-intercep, was 44.75 $(mg/L)^{-1}$. Because the plot between log q_e and log C_e from Eq. (4) did not give a straight line (not shown), the adsorption behavior could not be explained by Freundlich isotherm.

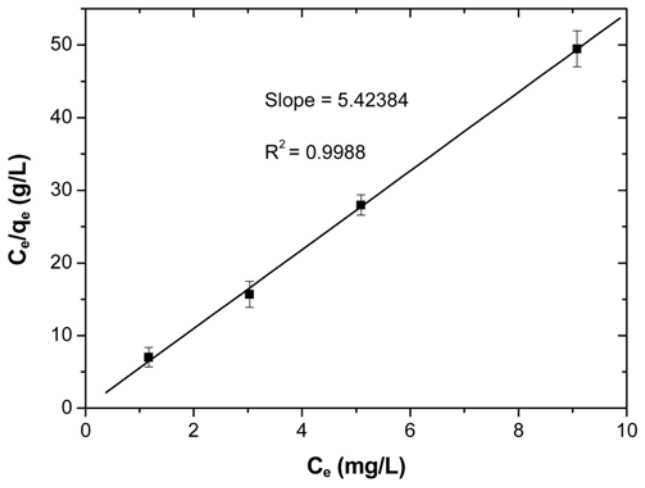

Fig. 8. Langmuir isotherm adsorption of methyl orange on TiO_2/RH-MCM-41; [cat.]=5 g/L, C_0=2, 4, 6 and 10 ppm, pH=4.5, [H_2O_2]=0.01 M.

CONCLUSIONS

Two catalysts containing 10 wt% Ti on RH-MCM-41 were synthesized: Ti-RH-MCM-41 synthesized by adding TBOT into the synthetic gel of RH-MCM-41 and TiO_2/RH-MCM-41 prepared by grafting TBOT on RH-MCM-41. Both catalysts showed characteristic of mesoporous structure with slightly less surface areas than the RH-MCM-41. The Ti(IV) cations in Ti-RH-MCM-41 had tetrahedral geometry, while in TiO_2/RH-MCM-41 were in anatase phase with octahedral geometry. The TiO_2/RH-MCM-41 was more active for photodegradation of methyl orange than Ti-RH-MCM-41. The optimum ratio between the weight of TiO_2/RH-MCM-41 to volume of methyl orange solution was 5 g/L and the optimum concentration of methyl orange was 2.0 ppm. The photocatalytic degradation of methyl orange on TiO_2/RH-MCM-41 obeyed pseudo-first order and the adsorption obeyed Langmuir isotherm.

ACKNOWLEDGMENT

Funding for this research was from the Synchrotron Light Research Institute (Public Organization) Grant 2-2548/PS01 and Suranaree University of Technology.

REFERENCES

1. H. Wang, J. Nui, X. Long and Y. He, *Ultrason. Sonochem.*, **15**, 386 (2008).
2. B. Neppolian, H. C. Choi, S. Sakthivel, B. Arabindoo and V. Murugesan, *Chemosphere*, **46**, 1173 (2002).
3. J. M. Hermann, *Catal. Today*, **53**, 115 (1999).
4. I. K. Konstantinou and T. A. Albanis, *Appl. Catal. B: Environ*., **49**, 1 (2004).
5. W. S. Nam and G. Y. Han, *Korean J. Chem. Eng*., **20**, 1149 (2003).
6. W. S. Nam and G. Y. Han, *Korean J. Chem. Eng*., **20**, 180 (2003).
7. A. Bhattacharyya, S. Kawi and M. B. Ray, *Catal. Today*, **98**, 431 (2004).
8. G. Li, X. S. Zhao and M. B. Ray, *Sep. Purif. Technol*., **55**, 91 (2007).
9. O. Carp, C. L. Huisman and A. Reller, *Prog. Solid. State. Chem.*, **32**, 33 (2004).
10. N. Grisdanurak, S. Chiarakorn and J. Wittayakun, *Korean J. Chem. Eng*., **20**, 950 (2003).
11. J. Wittayakun, P. Khemthong and S. Prayoonpokarach, *Korean J. Chem. Eng.*, **25**, 861 (2008).
12. P. Khemthong, S. Prayoonpokarach and J. Wittayakun, *Suranaree J. Sci. Technol.*, **14**, 367 (2007).
13. S. Loiha, S. Prayoonpokarach, P. Songsiriritthigun and J. Wittayakun, *Mater. Chem. Phys.*, **115,** 637 (2009).
14. D. Srinivas, R. Srivastava and P. Ratnasamy, *Catal. Today*, **96**, 127 (2004).
15. P. Schacht, L. Noreña-Franco, J. Ancheyta, S. Ramírez, I. Hernández-Pérez and L. A. García, *Catal. Today*, **98**, 115 (2004).
16. S. Bordiga, S. Coluccia, C. Lamberti, L. Marchese, A. Zecchina, F. Boscherini, F. Buffa, F. Genoni and G. Leofanti, *J. Phys. Chem.*, **98**, 4125 (1994).
17. Y. G. Shul, K. S. Oh, J. C. Yang and K. T. Jung, *J. Sol-Gel Sci. Tech-*

nol., **8**, 255 (1997).
18. M. Kitano**,** M. Matsuoka, M. Ueshima and M. Anpo, *Appl. Catal. A: Gen.*, **325**, 1 (2007).
19. M. Mrak, N. N. Tušar, N. Z. Logar, G. Mali, A. Kljajić, I. Arčon, F. Launay, A. Gedeon and V. Kaučič, *Micropor. Mesopor. Mater.*, **95**, 76 (2006).